Trans-mutation at Gold(III): A Mechanistic Study of a Catalytic Acetylene Functionalization via a Double Insertion Pathway

Marte Sofie Martinsen Holmsen,[†] Ainara Nova,[‡]* David Balcells,[‡] Eirin Langseth,[†#] Sigurd Øien-Ødegaard,[†] Richard H. Heyn,[§] Mats Tilset,[†‡]* Gábor Laurenczy[⊥]

[†]Department of Chemistry and [‡]Centre for Theoretical and Computational Chemistry (CTCC), Department of Chemistry, University of Oslo, P.O. Box 1033 Blindern, N-0315 Oslo, Norway

[§]SINTEF Materials and Chemistry, P.O. Box 124 Blindern, N-0314 Oslo, Norway

[⊥]Institut des Sciences et Ingénierie Chimiques, Ecole Polytechnique Fédérale de Lausanne, CH-1015 Lausanne, Switzerland

[#]Current address: SINTEF Materials and Chemistry, P.O. Box 124 Blindern, N-0314 Oslo, Norway

Corresponding authors: mats.tilset@kjemi.uio.no, ainara.nova@kjemi.uio.no

Abstract

The Au(III) complex $Au(OAc^F)_2(tpy)$ (OAc^F = $OCOCF_3$; tpy = 2-(*p*-tolyl)pyridine) catalyzes the *anti* addition of trifluoroacetic acid ($HOAc^F$) to acetylene to furnish vinyl trifluoroacetate. The Au(III) vinyl complex $Au(tpy)(OAc^F)(CH{=}CHOAc^F)$ (vinyl group bonded *trans* to tpy-*N*) is formed during the early stage of the reaction. The vinyl complex, which has been isolated and structurally characterized, resists protolytic cleavage of the vinyl group and therefore catalysis does not proceed by a simple formal insertion (*i.e.* coordination-nucleophilic attack-protolysis at the site *trans* to tpy-*N*) mechanism. Experimental evidence, including isotopic labeling, rather suggests that a double-insertion process is operative. The unobserved Au(III) divinyl complex $Au(tpy)(CH{=}CHOAc^F)_2$ is a crucial intermediate for which the true catalytic activity, comprising a coordination-nucleophilic attack-protolysis sequence, occurs at the site *trans* to tpy-*C*. The overall mechanism is in full agreement with DFT calculations and is a result of the considerable differences in the kinetic and thermodynamic *trans* effects of tpy-*N* vs. tpy-*C* on each reaction step. The computational data provide a rationale for the catalytic functionalization of acetylene *trans* to tpy-*C*, whereas

ethylene (previously reported) only undergoes a stoichiometric insertion, and then comes to a full stop, *trans* to tpy-*N*.

Keywords:

Acetylene functionalization

Cyclometalated complexes

Au(III) catalysis

Au(III) vinyl complexes

DFT calculations

Reaction mechanisms

Trans effects

INTRODUCTION

The functionalization of alkenes and alkynes under mild conditions is of great practical and economic interest because readily available hydrocarbons may be converted to value-added products. Such processes may be catalyzed by a plethora of metals and metal complexes, and gold is especially recognized and attractive due to its ability to π-coordinate alkenes and alkynes, causing them to be activated towards nucleophilic attack.[1-17] This has given rise to a virtual explosion in the use of gold complexes to catalyze the chemical transformation of alkenes, alkynes, and other unsaturated compounds during the last decade. The use of gold complexes quickly matured to find applications in the catalytic transformations of multiply functionalized precursors to complex organic structures. Less attention has been paid to elucidate the details of the reactivities of the smallest alkenes and alkynes, i.e. ethylene and acetylene, at gold complexes.

Acetylene has become less utilized as a potential C_2 building block for production of commodity chemicals due to the availability of less expensive hydrocarbons from petrochemical feedstocks. However, vinyl chloride is produced in China on a large scale by acetylene hydrochlorination, with the use of mercury catalysts.[18,19] The use of mercury raises obvious environmental concerns, and alternatives are thus considered. This has led to attempts at developing analogous chemistry using supported gold catalysts. The acetylene hydrochlorination process, described by Hutchings and coworkers and others, is a classic case in this regard.[18-23] Mechanistically, Hutchings and coworkers have proposed on the basis of experiments and computations, that a coordination-nucleophilic attack mechanism, analogous to that in Scheme 1, path A is operative. For the hydrotrifluoroacetylation of acetylene, mercury based processes have been described in the patent literature,[24,25] but to our knowledge, no Au catalyzed process has been reported.

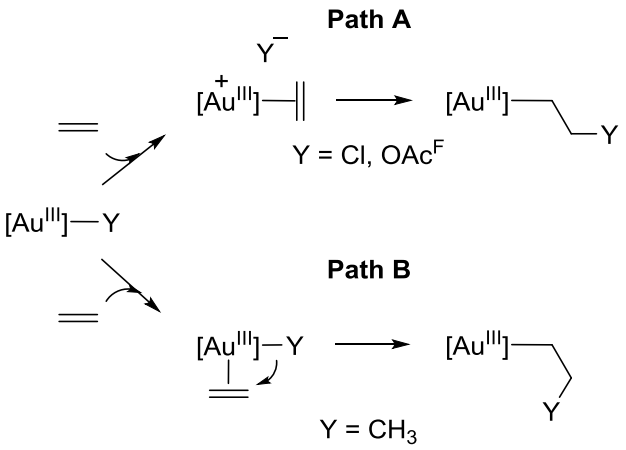

Scheme 1. Possible pathways for the insertion of an olefin into a $[Au^{III}]$-Y bond (Y = Cl, OAc^F, CH_3; OAc^F = $OCOCF_3$).

Although the differences between Au(I) and Au(III) catalysis can be profound,[26] studies on Au(I) continue to strongly dominate the field, in part due to the relative paucity of efficient and robust protocols for preparation of Au(III) complexes. Bi- and tridentate ligands, including cyclometalated ones, have proven particularly useful to support Au(III) species.[27-30] Catalytic transformations involving Au(I)/Au(III) redox cycles for effecting C-C and C-heteroatom bond forming reactions at alkenes and alkynes have attracted considerable recent attention,[31-36] including alkyne functionalization with Selectfluor.[31,37-42]

The intermediacy of Au(III) alkene and alkyne complexes in these catalytic transformations is evident. Nevertheless, there has to date appeared only one report[43] of a structurally characterized Au(III) alkene complex, $AuMe_2(cod)^+$, and two additional reports on the isolation and/or NMR observation of Au(III) alkene complexes that are supported by formally dianionic, C^N^C pincer-type ligands.[44,45] Au(III) alkyne complexes remain elusive, although such species are frequently invoked in catalytic and stoichiometric transformations and have been explored by computational means.[46,47] We recently reported a theoretical study of the detailed bonding, electronic structures, and reactivity patterns of simple Au(III) model compounds of the type $AuX_3(L)$ and $AuX_2(L)_2^+$, where L = C_2H_4 or C_2H_2, and X = H, Me, or Cl.[15]

The mechanism for the insertion of ethylene into an Au-O bond of $Au(tpy)(OAc^F)_2$ (**1**; tpy = 2-(*p*-tolyl)pyridine, Scheme 2) was explored by our group by combining experiments and DFT calculations.[48] This non-oxidative functionalization of ethylene which leads to C-heteroatom bond formation proceeds mechanistically as a *formal* insertion *via* ethylene coordination followed by attack by external nucleophile (Scheme 1, path A), as opposed to

the C-C bond forming coordination-insertion reactions recently investigated, experimentally and computationally, by Bourissou and coworkers[45,49-51] (Scheme 1, path B). Similar formal insertions have been reported by the groups of Atwood[52] and Bochmann.[44] Selective insertion of ethylene into the Au-O bond *trans* to N of the chelating tpy ligand furnished Au(tpy)($CH_2CH_2OAc^F$)(OAc^F) (**2**, Scheme 2). Although the *trans* to tpy-*C* coordination site is kinetically more accessible, the *trans* to tpy-*N* insertion product is thermodynamically favored. Unfortunately, a catalytic process could not be achieved with this system, because protolytic cleavage of the Au-C(sp^3) bond in **2** does not occur.

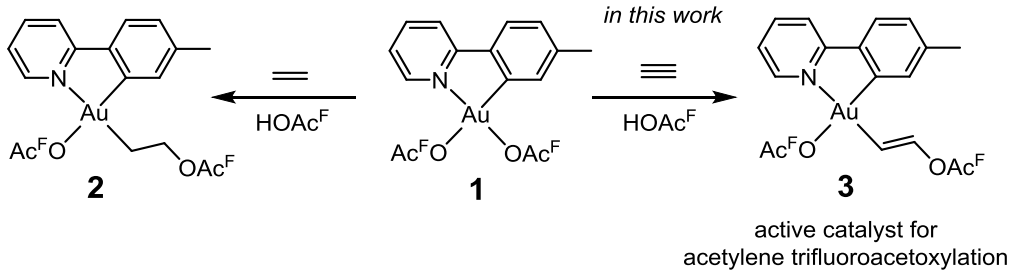

Scheme 2. Formal insertion of ethylene and acetylene at Au(OAc^F)$_2$(tpy).

In this paper, we report that Au(tpy)(OAc^F)$_2$ (**1**), in contrast to its stoichiometric reactivity towards ethylene, causes the catalytic formation of vinyl trifluoroacetate by the *anti* addition of trifluoroacetic acid, $HOAc^F$, to acetylene. A detailed, combined experimental and computational study unravels an unexpected complexity in this catalytic transformation. The combined evidence suggests that this reaction proceeds *via* a double insertion pathway, in which the first acetylene inserted product (**3**; Scheme 2) is the active catalyst involving an unobserved Au(III) divinyl species as a crucial intermediate. The potential feasibility of an analogous reaction pathway with ethylene as the substrate has also been analyzed.

RESULTS AND DISCUSSION

Reactions of Au(tpy)(OAc^F)$_2$ with Acetylene. When acetylene was bubbled through a solution of **1** in trifluoroacetic acid-*d* (DOAc^F) at ambient temperature and pressure, an immediate reaction occurred. A ^{1}H NMR spectrum (Figure S21, ESI) acquired less than 5 min after mixing revealed that ca. 50% of **1** had reacted to furnish the vinyl complex Au(tpy)(OAc^F)(CH=CHOAc^F) (**3**) (Scheme 3). The complete ^{1}H NMR spectra (*vide infra*) of **3** established that the formal insertion of acetylene into one of the Au–O bonds has taken place selectively *trans* to tpy-*N* and in an *anti* fashion. This parallels the selectivity features of the ethylene insertion at **1** previously described.[48] In addition, signals due to the vinyl protons in (*E*)-vinyl trifluoroacetate-*d* (**4-*d***) (δ 5.19 and 7.18, mutually coupled with *trans* $^3J_{HH}$ = 13.6 Hz) were seen. The yield of **4-*d***, determined from NMR integration against an internal standard, was ca. 20% based on the initial amount of **1**. Finally, traces of (1*E*,3*E*)-1,4-bis(trifluoroacetoxy)-1,3-butadiene (**5**) and D_2tpy^+ were detected. It will be seen that **4-*d*** production is catalyzed by Au(III) and that **5** and D_2tpy^+ results from catalyst deactivation, initiated by protolytic cleavage of the Au-C and Au-N bonds of the Au(tpy) moiety.[43] After 30 min, all of **1** had reacted and **3** was the only Au(tpy)-containing species seen in solution. The yield of **4-*d*** (NMR integration) now corresponded to ca. 200%, based on the initial amount of **1**. NMR signals due to **5** had grown in prominence (ca. 40% of the quantity of **3**). The amount of D_2tpy^+ had increased to ca. 50% of the quantity of **3**. The reaction was monitored by ^{1}H NMR for 24 h, at which time **4-*d*** (along with traces of **4**), **5**, and D_2tpy^+ were the only species that could be detected and all **3** had decomposed. At this point, D_2tpy^+ and **5** had formed in essentially quantitative yields. No other significant changes occurred after extended reaction times. The estimated turnover numbers for production of **4-*d***, based on integration of the NMR signals of **4-*d*** against the signal of an internal standard in multiple experiments, were 13-15 per Au (see Table S1, ESI). A control experiment established that no reaction occurred between acetylene and DOAc^F in the absence of **1** or other sources of Au on the time scale of these reactions. Clearly, Au species must be involved in what amounts to a catalytic transformation of acetylene into vinyl trifluoroacetate.

In a complementary experiment, **1** was treated with acetylene and non-deuterated trifluoroacetic acid, HOAc^F, in CD_2Cl_2 (CD_2Cl_2: HOAc^F, 6:1 (v:v)), and the same products were qualitatively formed; as expected, **4** and H_2tpy^+ were now formed with no D incorporation. The highest turnover numbers (21-24; see Table S1, ESI) were obtained in this solvent mixture when acetylene was added at 0 °C before the reaction was monitored at

ambient temperature. This may be a result of combined effects of increased acetylene solubility, larger production of **3**, and possibly slower rates of catalyst deactivation at the lower temperature.

The identity of **4** was confirmed by ^{1}H NMR analysis of a product mixture that was spiked with a commercial sample. The disubstituted butadiene **5** has neither been isolated nor been previously described, but its identity was inferred from the ^{1}H NMR spectrum as well as COSY spectra. The ^{1}H NMR spectrum of **5** exhibited a well-defined signal, attributed to the protons β to OAc^{F}, with a rather complicated splitting pattern at δ 6.30 in $DOAc^{F}$ (δ 6.35 in CD_2Cl_2, see Figures S22 and S25, ESI). A ^{1}H–^{1}H COSY experiment (Figure S24, ESI) demonstrated that this signal couples with another signal, attributed to the protons α to OAc^{F}, further downfield at ca. δ 7.4 in $DOAc^{F}$ (δ ca. 7.5 in CD_2Cl_2). Although the latter in part overlaps with signals from the tpy ligand, the signal appears to have the same intensity and symmetrical appearance as the one at δ 6.30. The observed spectrum, in particular the splitting pattern, strongly resembles that of the non-fluorinated analogue of **5**, (1*E*,3*E*)-1,4-diacetoxy-1,3-butadiene (see Figure S27, ESI).

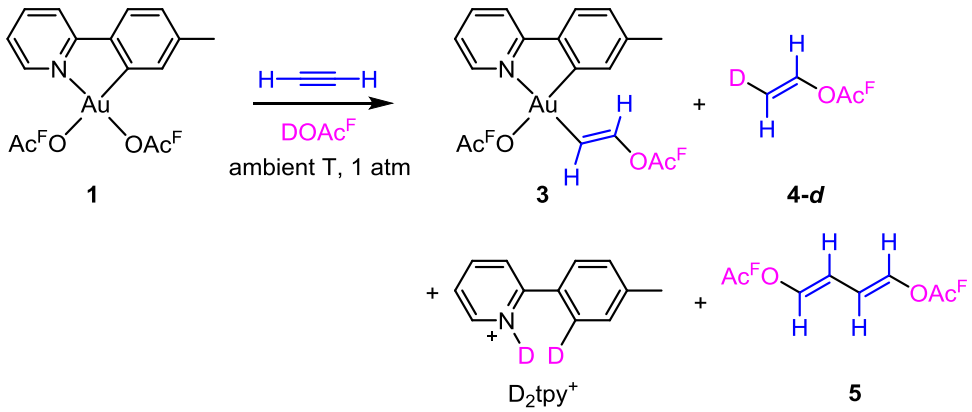

Scheme 3. Reaction between **1** and acetylene in $DOAc^{F}$ (OAc^{F} = $OCOCF_3$). See text for details.

Preparation and Spectroscopic and Structural Characterization of the Acetylene Insertion Product 3. No Au(III) π-coordinated acetylene complex could be observed by ^{1}H NMR during these reactions, neither at room temperature nor upon lowering the temperature to -60 °C in CD_2Cl_2. A hypothetic acetylene π-complex must therefore be promptly captured by $HOAc^{F}$ or $^{-}OAc^{F}$ to furnish **3**. This vinyl complex appears to be a plausible intermediate in the catalytic cycle, as a protolytic cleavage of its vinyl group with $HOAc^{F}$ would produce vinyl trifluoroacetate. This would regenerate **1** and close the rather simple, putative catalytic cycle depicted in Scheme 4. The diene **5** as well as H_2tpy^{+} would result from catalyst

decomposition under the acidic conditions. In order to investigate the possibility of this mechanism, we sought to isolate and further investigate the observed insertion product **3**.

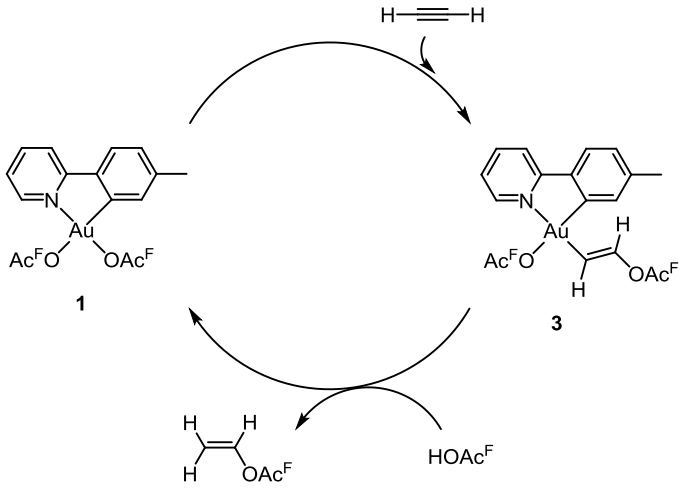

Scheme 4. Simplified, putative catalytic cycle for the trifluoroacetylation of acetylene.

When acetylene was bubbled through a solution of **1** in $HOAc^F$ at 0 °C, the insertion reaction still proceeded smoothly, whereas the catalytic production of vinyl trifluoroacetate proceeded at a considerably slower rate. From the resulting solution, the insertion product **3** was isolated in moderate (40-42%) yields (Scheme 5).

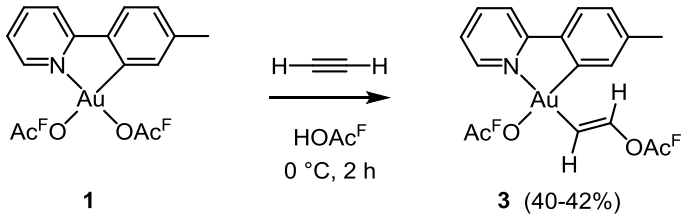

Scheme 5. Synthesis of Au(III) vinyl complex **3**.

The ^1H NMR spectrum of isolated **3** was in perfect agreement with that observed in the NMR-scale experiments. The formal insertion of acetylene *trans* to tpy-*N* was supported by a ^1H–^1H NOESY experiment which revealed a clear NOE correlation between the vinylic proton α to Au (δ 6.43) and the proton β to Au (δ 7.31) in the tolyl part of the tpy ligand (proton $H^{6'}$ in ESI, Figure S8). The ^{19}F NMR spectrum of **3** in dichloromethane-d_2 showed two well-defined, sharp peaks at δ(^{19}F) = –77.1 and –77.5 (Figure 1, top). A ^{19}F–^1H HOESY experiment showed that the δ –77.1 signal arises from the OAc^F ligand *trans* to tpy-*C* (See ESI, Figure S10). Addition of ca. 1 equiv of $HOAc^F$ to the solution caused the signal at δ –77.1 to undergo significant broadening, whereas free $HOAc^F$ gave rise to a broadened signal at δ –78.2 (Figure 1, bottom). This broadening suggests the kinetic availability of the coordination site *trans* to tpy-*C* and exchange of this OAc^F ligand with free trifluoroacetic

acid. These spectroscopic features are in close agreement with those of the ethylene insertion product, **2**.[48] Furthermore, our previous investigation of **1** by ^{19}F NMR demonstrated that the OAc^F ligand *trans* to tpy-*C* exclusively undergoes fast and reversible dissociation in polar media on the NMR time scale.[48] Thus, a kinetic labilization of the OAc^F ligands trans to tpy-*C* are consistently seen in **1**, **2**, and **3**, in accord with a greater kinetic *trans* effect of tpy-*C* than tpy-*N*. Importantly, this provides an additional coordination site for incoming substrates. Our recent report on a metallacycle formation from **1**, where both the *trans* to tpy-*C* and the *trans* to tpy-*N* coordination sites are utilized to incorporate ethylene, acetonitrile, and water, corroborates the availability of this site.[53]

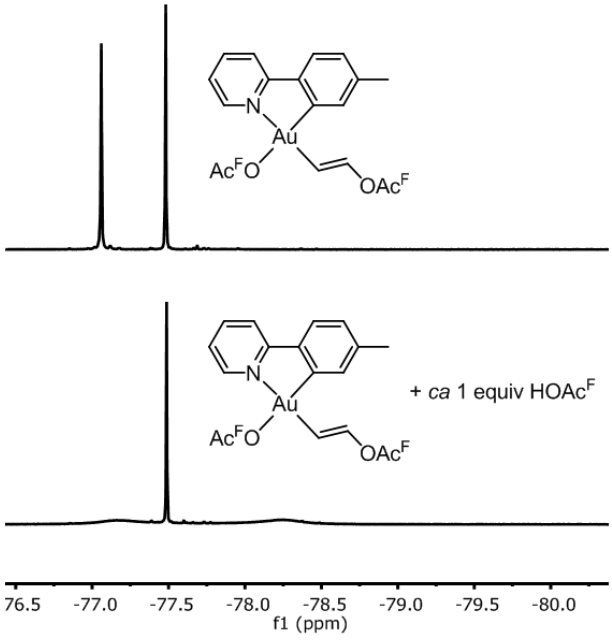

Figure 1. ^{19}F NMR (188 MHz, CD_2Cl_2) spectra of Au(III) vinyl complex **3**: (Top) Spectrum of solution of **3** alone. (Bottom) Spectrum of solution of **3**, after addition of ca. 1 equiv of $HOAc^F$.

Although Au(III) vinyl species are invoked as plausible intermediates in Au(III) mediated reactions,[54] there is still a paucity of well-characterized Au(III) vinyl complexes,[55-59] only three of which have been structurally characterized.[55,57] Therefore, the molecular structure of **3** was determined by a single-crystal X-ray diffraction analysis. An ellipsoid plot of the structure is shown in Figure 2, along with selected metrical parameters. Detailed crystallographic data and metrical parameters are given in the ESI.[60] The crystal structure contains two molecules (of which only one is shown in Figure 1) in the asymmetric unit, and also exhibits open channels which contain disordered solvent molecules. The two molecules in the asymmetric unit are almost identical and related by pseudosymmetry (see below and ESI). The complex exhibits the slightly distorted square planar coordination geometry that is

anticipated for a d^8 Au(III) complex, with angular distortions in the square plane as expected for the 5-membered ring chelate structure. Importantly, the molecular structure shows that the formal insertion has occurred *trans* to tpy-*N* and with a *trans* (*E*) geometry of the resulting vinyl group, in full agreement with the conclusions based on the NMR analysis. The 7.3° deviation of the C101–Au10–N101 bond angle in the tpy chelate from the idealized 90 to 82.7(5)° and the Au-ligand distances Au10–N101, Au10–C101, and Au10–O101 are within the ranges that have previously been reported by us for the related complexes Au(tpy)$(OAc^F)_2$,[61] Au(tpy)Me_2,[61] Au(tpy)$(CH_2CH_2OAc^F)(OAc^F)$,[48] Au(tpy)-$(CH_2CH_2OCH_2CF_3)(OAc^F)$,[48] and the recently reported metallacycle.[53] The Au–C(sp^2) bond distance to the vinyl group, Au10–C113, is 2.027(13) Å which is slightly shorter than the Au–C(sp^3) bond distances *trans* to tpy-*N* in the related complexes, but in the range (2.004(19)-2.043(4) Å) for Au–C(sp^2) bonds in structurally characterized Au(III) vinyl species.[55,57] The C113–C114 bond distance of 1.293(19) Å is rather close to typical distances in disubstituted C=C double bonds (*trans* 1,2-disubstituted alkenes, averaging 1.312(11) Å[62]), and is the shortest C=C bond distance in structurally characterized Au(III) vinyl complexes (range 1.311(3)-1.344(6) Å).[55,57] The structure of **3** displays parallel, displaced π–π stacking along the *b* direction, and the relatively short distance between the parallel planes of the tpy ligands alternates between 3.41 and 3.43 Å for the two asymmetric units.

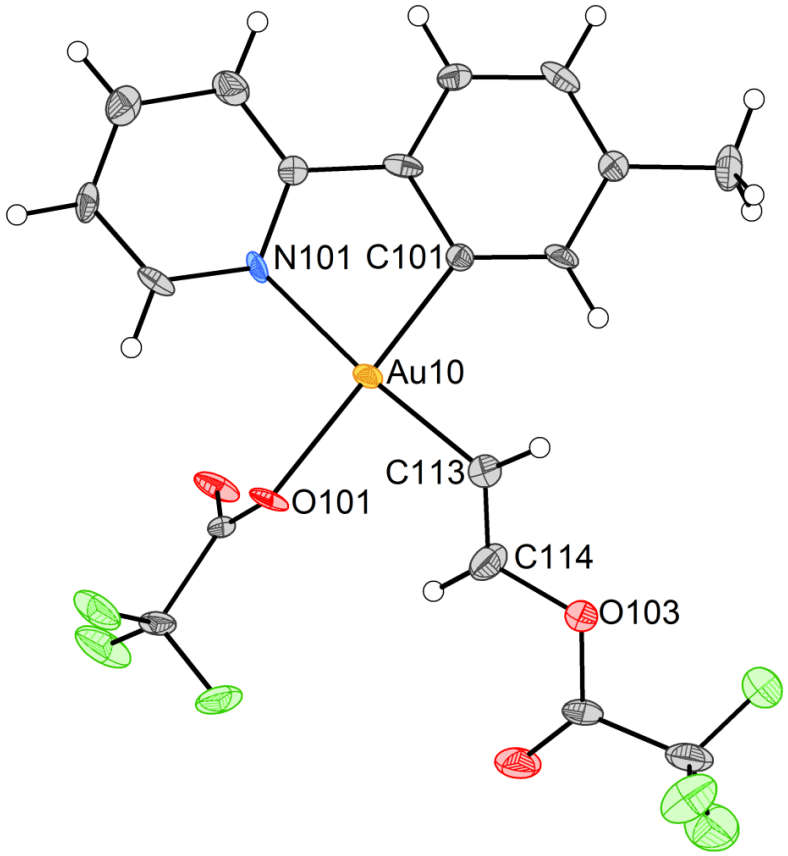

Figure 2. ORTEP drawing of Au(III) vinyl complex **3**, with 50 % probability ellipsoids. Selected bond distances [Å] and angles [°]: Au10-N101, 2.070(11); Au10-C101, 2.007(11); Au10-O101, 2.110(8); Au10-C113, 2.027(13); C113-C114, 1.293(19); C114-O103, 1.450(18); N101-Au10-O101, 96.5(4); C101-Au10-N101, 82.7(5); C101-Au10-C113, 92.2(5); C113-Au10-O101, 88.6(5); C101-Au10-O101, 179.0(4); C113-Au10-N101, 173.2(5); Au10-C113-C114, 123.2(11); C113-C114-O103, 115.3(14); Au10-C113-C114-O103, 175.7(9). Disordered solvent molecules are omitted for clarity. The asymmetric unit consists of two complexes, and the metrical parameters are given for the complex with the lower uncertainties in the bond distances and bond angles.

On the Involvement of the Acetylene Insertion Product 3 in the Catalytic Reaction. The successful isolation of the vinyl complex **3** offered unique possibilities to check whether it is indeed an intermediate in the proposed catalytic cycle (Scheme 4). If this were the case, each of the reaction steps – insertion and protolytic cleavage – should proceed at rates that are in accord with the turnover rates of the catalysis. Furthermore, it should be possible to access the same catalytic cycle starting with either **1** or **3**. Since **1** and **3** coexisted in solution during catalysis starting with **1**, both species ought to coexist under approximate steady-state conditions after a few turnovers if catalysis according to Scheme 4 is also initiated with **3**.

We were therefore surprised when it was found that a solution of the isolated vinyl complex **3** in $DOAc^F$ in the *absence* of acetylene was remarkably stable. Even after days at ambient temperature, there was no hint of conversion of **3** into the expected product of

protolytic cleavage, **1**; **4-*d*** could also not be detected. This observation appears to rule out the simple catalytic mechanism in Scheme 4.

Interestingly, when the solution of **3** in neat $DOAc^F$ (or in CD_2Cl_2:$HOAc^F$, 6:1 (v:v)) was again exposed to acetylene by bubbling through the solution, catalysis ensued; vinyl trifluoroacetate now formed catalytically (estimated turnover numbers after 24 h, ca. 11-12 (12-15 in CD_2Cl_2/$HOAc^F$). Importantly, under these catalytic reaction conditions there was no hint by ^{1}H NMR of **1** or other intermediates – again, seemingly ruling out the mechanism in Scheme 4. The reaction was monitored by ^{1}H NMR until the catalytic activity ceased. At this point, in addition to NMR signals arising from the D_2tpy^+, the tell-tale spectroscopic signatures of the decomposition product **5** were seen (see Figures S22 and S25).

Formation and Characterization of an Au(III) C-bonded Enolate and its Involvement in the Catalytic Reaction. We were intrigued by the observation of the disubstituted butadiene **5** after extended reaction times in the catalytic reaction of **1** with acetylene. The four-carbon chain of **5** must arise from coupling of two acetylenic C_2 units. The possible involvement of **1**, **3**, **4**, and acetylene all appeared possible. In order to probe for the involvement of **4**, a solution of **1** in $HOAc^F$ was treated with 10 equiv of **4**. A slow reaction ensued which, however, gave no detectable quantities of **5** or any other four-carbon coupling products. Instead, during the course of six days a clean transformation of **1** to the C-bonded Au(III) enolate complex **6** (Scheme 6) occurred, without observable intermediates. This new complex, isolated in 51-60% yield, exhibited a clear NMR fingerprint, with one signal at δ 9.92 (t, J = 4.6 Hz) for the formyl proton, and the other at δ 3.14 (d, J = 4.6 Hz) for the methylene group. When **6** was dissolved in $DOAc^F$, ^{1}H NMR analysis revealed that H/D exchange between the deuterated solvent and the methylene group occurred, presumably via keto/enol tautomerization, evidenced by a decrease of the signal intensity for the methylene group with an approximate half-life of 25 min under these conditions. This was accompanied by apparent loss of coupling and the conversion of the formyl triplet signal into a singlet (see ESI, Figure S20). The mechanism of formation of **6** remains uncertain and has not been further investigated, but may involve the formal insertion of vinyl trifluoroacetate at **1** followed by elimination of trifluoroacetic anhydride. Subsequently, it was found that **6** also can be obtained from vinyl complex **3**, simply by a hydrolysis reaction in the presence of $HOAc^F$.

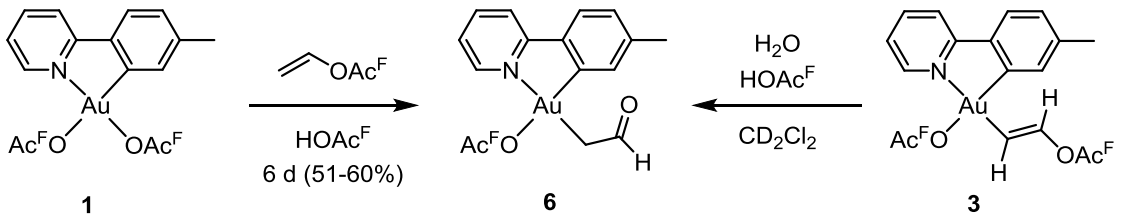

Scheme 6. The two routes for generating Au(III) enolate complex **6**.

The rather unexpected enolate complex **6** was subjected to a single-crystal X-ray diffraction analysis. An ellipsoid plot of the molecular structure of **6** is shown in Figure 3, along with selected metrical data. Detailed crystallographic data and metrical parameters are given in the ESI. The molecular structure verifies the presence of the enolate ligand *trans* to tpy-*N*, in agreement with the NMR data. The OAc^F ligand is disordered over two well-defined positions (see Figure S36, ESI). Two closely related Au(III) acetonate complexes, (phenylpyridine)Au(X)(CH_2COMe) (X = Cl or NO_3; CH_2COMe *trans* to ppy-*N*), have been structurally characterized.[63] Complex **6** also exhibits a slightly distorted square planar coordination geometry, with a 5-membered ring chelate bond angle of 81.69(9)°. The Au-ligand distances Au1–N1, Au1–C1, and Au1–O2 are again within the ranges that have been observed in the related Au(III)-tpy complexes.[48,53,61] The Au–C(sp^3) bond distance, Au1–C13, is 2.069(2) Å which is somewhat longer than the Au–C(sp^3) bond distances *trans* to tpy-*N* in our Au(III)-tpy complexes (range 2.038(4)-2.042(3) Å) and quite similar to those observed in the Au(III) acetonate complexes (2.067(7) Å for X = Cl and 2.059(5) Å for X = NO_3[63]). The C13–C14 bond (1.468(3) Å) and the C14–O1 double bond (1.212(3) Å) distances are rather close to the corresponding distances in aldehydes, 1.510(8) Å and 1.192(5) Å, respectively.[62] The crystal structure displays parallel, displaced π–π stacking along the *b* direction, with a distance between the parallel planes of 3.485 Å.

Interestingly, it was found that the enolate complex **6**, when dissolved in $DOAc^F$, also catalyzed the addition of $DOAc^F$ to acetylene (ca. 7 turnovers, 24 h). During this reaction, substantial decomposition to form unidentified products occurred.

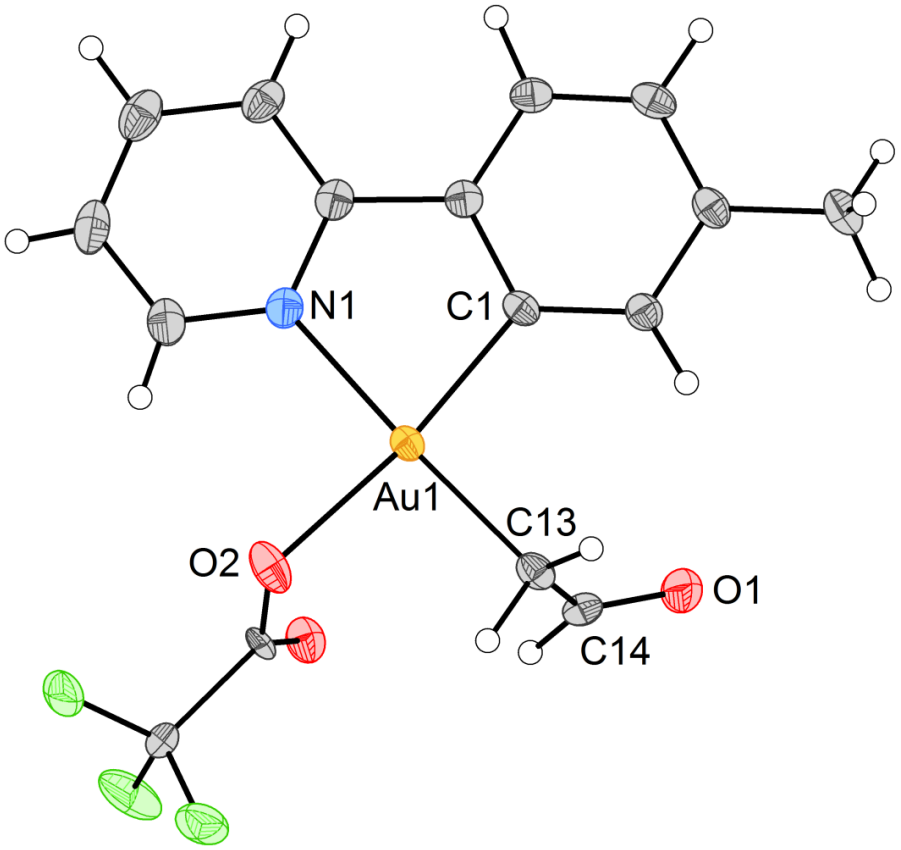

Figure 3. ORTEP drawing of Au(III) C-bonded enolate complex **6**, with 50 % probability ellipsoids. Selected bond distances [Å] and angles [°]: Au1-N1, 2.090(2); Au1-C1, 2.006(2); Au1-O2, 2.1016(17); Au1-C13, 2.069(2); C13-C14, 1.468(3); C14-O1, 1.212(3); N1-Au1-O2, 91.19(8); C1-Au1-N1, 81.69(9); C1-Au1-C13, 95.22(9); C13-Au1-O2, 91.90(8); C1-Au1-O2, 171.73(8); C13-Au1-N1, 176.91(8); Au1-C13-C14, 108.68(16); C13-C14-O1, 125.8(2); Au-C13-C14-O1, 111.9(2). The OAc^F *trans* to C1 is disordered (see ESI).

A Double Insertion Mechanism for Catalysis? The experimental results described thus far have demonstrated that in addition to **1**, the two complexes **3** and **6**, with -CH=CHOAc^F or -CH_2CHO *trans* to tpy-*N*, respectively, were catalytically active, with no detectable intermediates in the case of **3**. This led us to surmise that the "real" catalytic site actually might be the kinetically available coordination site *trans* to tpy-*C*, and that the apparent catalysis by **1** occurred only *via* its initial transformation to **3**. Further support for this was obtained when Au(tpy)(NTf_2)(Me), prepared *in situ* by treatment of previously described[64] Au(tpy)(Br)(Me) with $AgNTf_2$, was seen to cause the formation of vinyl trifluoroacetate from acetylene in $HOAc^F$ (albeit only ca. 1 turnover, during 15 h), again with no detectable intermediates by ^{1}H NMR. Also in this case, several other unidentified products were obtained; no attempts were made to elucidate this any further.

The experimental results therefore led us to postulate a modified reaction mechanism for the catalysis. Scheme 7 shows a double-insertion mechanism that appears to be consistent

with experimental results described thus far. Here, the first insertion (a) generates the vinyl complex **3** which, consistent with observations, does *not* undergo protolytic cleavage (b). Instead, a second insertion (c) provides an unobserved divinyl complex **7** which undergoes protolytic cleavage of the vinyl group *trans* to tpy-*C*, furnishing vinyl trifluoroacetate with concomitant regeneration of catalytically active **3**. Thus, the catalytic cycle involves **3** and **7**, whereas **1** merely acts as a precatalyst. The unobserved divinyl complex **7** would nicely account for the formation of **5** via a reductive elimination pathway.

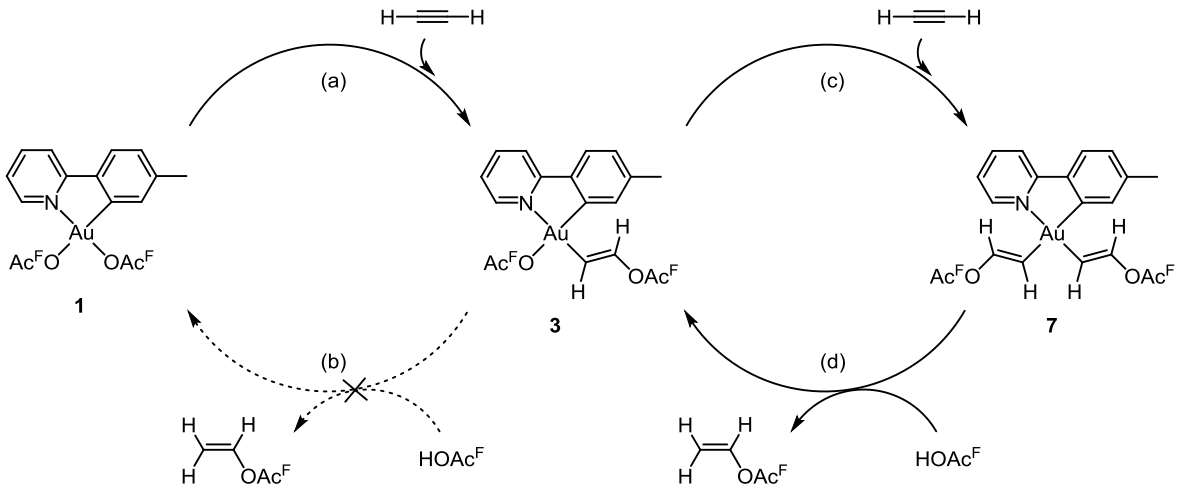

Scheme 7. Double insertion mechanism for the trifluoroacetylation of acetylene catalyzed by **3**, with **1** acting as a precatalyst.

In order to experimentally test the proposed double-insertion hypothesis by ^{1}H NMR, a labelling experiment was designed (Scheme 8a). If the double insertion pathway operates, then the reaction of **3** with acetylene-d_2 in HOAc^F should provide vinyl trifluoroacetate-d_2, (*Z*)-CHD=CD(OAc^F) (**4-*d*$_2$**), from catalysis *trans* to tpy-*C* during all catalytic cycles including the first one. In contrast, catalysis *trans* to tpy-*N* would furnish non-deuterated vinyl trifluoroacetate during the first cycle, then dideuterated during following cycles. Acetylene-d_2 was prepared from CaC_2 and D_2O by adaption of a reported procedure.[65] When acetylene-d_2 was bubbled through a solution of **3** in HOAc^F, **4-*d*$_2$** was formed as the dominant product during the first turnover, as inferred from the appearance of a broad singlet at the chemical shift δ 4.96 for the proton located *trans* to the OAc^F group in vinyl trifluoroacetate. There was no indication of vinyl trifluoroacetate-d_0 (**4**), which might arise from protolytic cleavage of the Au-vinyl bond in **3**, during the first and most diagnostic turnover. However, after the first turnover and more extensive reaction times, acetylene-d_1 and d_0 were seen to slowly form giving rise to concomitant generation of **4-*d*$_1$** and non-deuterated **4**, presumably due to D/H exchange on acetylene in solution or π-bonded at Au. Thus, strong support is provided to the proposed double-insertion catalytic pathway, in which the catalysis actually occurs *trans* to

tpy-*C* (Scheme 7, rightmost cycle), and not *trans* to tpy-*N* as might be anticipated at first glance. The occurrence of some residual reactivity in the position *trans* to tpy-*N* cannot be excluded completely.

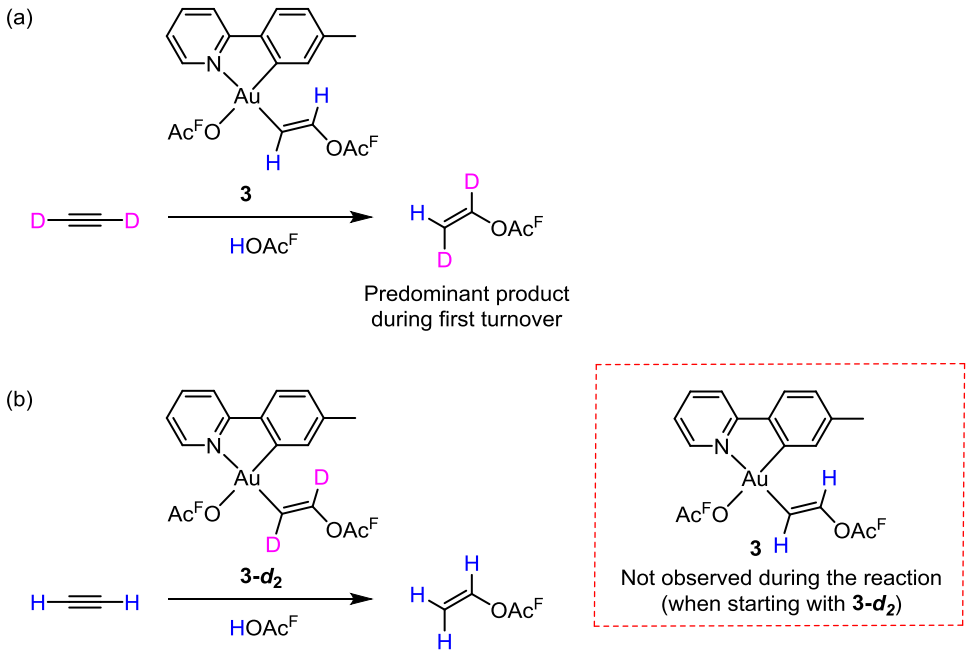

Scheme 8. Deuterium labelling experiments corroborate catalysis *trans* to tpy-*C*.

Due to the mentioned complications of the (presumably Au(III)-promoted) D/H exchange on acetylene, a complementary experiment was performed which circumvented this problem. When **3-*d*$_2$** was reacted with acetylene-d_0 in the presence of HOAc^F, no evidence for formation of unlabeled **3** was seen at any time of the reaction, neither during the first turnover nor later (Scheme 8b). This suggests that no protolytic cleavage of the Au-vinyl bond *trans* to tpy-*N* occurs, and that no subsequent insertion of acetylene-d_0 has occurred at this position. Furthermore, signals arising from **5** were observed also in this reaction (δ 6.35 and ca 7.5); however, the splitting pattern of the δ 6.35 signal due to the proton β to OAc^F was now simplified to resemble a doublet of triplets with a *trans* $^3J_{HH}$ coupling of 12.2 Hz and $^3J_{HD}$ coupling of 1.4 Hz, and the partially overlapping signal due to the proton α to OAc^F resembled a doublet (ESI, Figure S26). This suggests that **5-*d*$_2$** had formed by a reductive elimination of one vinyl-d_2 group *trans* to tpy-*N* and one vinyl-d_0 group *trans* to tpy-*C*.

The finding that **3**, **6**, as well as the methyl analogue Au(tpy)(NTf$_2$)(Me) all catalyze the formation of vinyl trifluoroacetate is now readily rationalized in that catalysis proceeds *via* coordination of acetylene, nucleophilic attack by $^-$OAc^F and protolysis *trans* to tpy-*C*. By virtue of the considerably greater *trans* effect of tpy-*C* (an aryl group) than tpy-*N* (pyridine),

hydrocarbyl groups bonded *trans* to the tpy-*C* site should be more prone to protolytic cleavage than groups bonded *trans* to tpy-*N*. Differences in thermodynamic and kinetic *trans* effects of tpy-*C vs*. tpy-*N* have been observed and discussed previously;[66] here, these effects prove to be crucial for catalytic reactions of acetylene. These effects will be further discussed in the context of DFT calculations of the mechanism (*vide infra*).

In view of the proposed mechanism, the formation of **5** and D_2tpy^+ is readily accounted for as catalyst deactivation products, arising from the divinyl complex **7** (Scheme 9). We recently reported that Au(tpy)Me_2 undergoes protolytic cleavage already at –78 °C.[43] The protolysis caused the selective cleavage of the Au–C(tpy) bond, which was followed by reductive elimination of ethane from the resulting putative 3-coordinate intermediate; Au–Me protolysis was not observed at all. If **7** behaves analogously, the 3-coordinate specie in the middle of Scheme 9 would be generated, and reductive elimination of the two vinyl groups would furnish **5,** followed by complete decomposition and formation of H_2tpy^+ and Au(s) (the mode of eventual Au(s) formation from Au(I) is unknown). Apparently, protolytic cleavage of the Au–Me bonds in Au(tpy)Me_2 is kinetically disfavored relative to the cleavage of the Au–C(tpy) bond, reflecting a preference for protolysis of Au–C(sp^2) bonds. On the other hand, protolysis at **7** may occur competitively at two Au–C(sp^2) bonds. Of these, protolysis of Au–C(vinyl) *trans* to tpy-*C* must be favored over protolysis at Au–C(tpy). This is required in order for catalysis to be kinetically preferred over deactivation. The *trans* effects of tpy-*C vs*. tpy-*N* causes protonation of Au–C(vinyl) *trans* to tpy-*N* to be even slower.

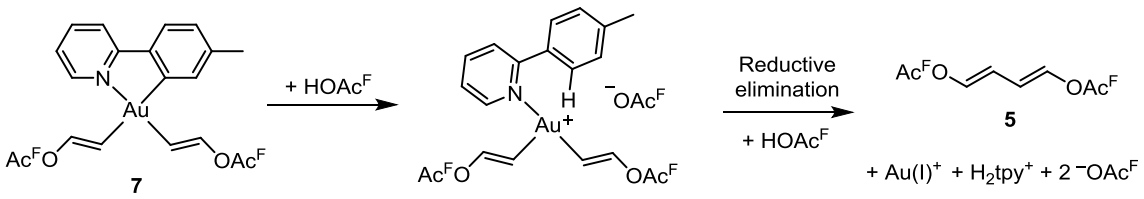

Scheme 9. Suggested decomposition pathway for the divinyl complex **7** furnishing **5**.

Nanoparticle Involvement? The results discussed so far are readily interpreted in terms of the proposed double insertion pathway. Nevertheless, there is always a concern that catalysis may be effected by Au nanoparticles,[67,68] whether originally present as a low-level contaminant, or as a result of catalyst decomposition. Decomposition eventually occurred in the systems described, and during the reaction a dark brown to black precipitate appeared which is probably Au particles. This is particularly relevant, considering the activity of metallic gold as a catalyst for vinyl chloride production from acetylene and HCl.[19,21] Whereas

it is readily envisaged that Au particles may be active catalysts also in our system, this scenario does not appear to rationalize the results of the mechanistic investigation. In particular, the compelling evidence gained from the labeling experiments support the notion of a process catalyzed by molecular complexes. Nevertheless, a series of control experiments were conducted in order to assess to what extent Au particles might be involved. The Au particles originating from the catalyst decomposition were isolated and their reactivity was investigated under the same reaction conditions as described for the homogeneous system. Upon comparing the outcome of these experiments with the homogenous system, it was found that the Au particles may be responsible for maximum ca. 4-13% of the total production of **4**. Full details of these control experiments are given in the ESI.

DFT Calculations: Reaction Mechanism.

A computational study of the catalytic trifluoroacetoxylation of acetylene with **1** was performed using DFT (PBE0-D3/SDD(f),6-311+G**, with structures optimized in solvent with the continuum SMD model; see Computational Details) calculations to test the mechanistic proposal shown in Scheme 7, and to provide additional insight into the different reactivity of acetylene and ethylene. Following our previous work[48] on the ethylene insertion into the Au–OAc^F bond in Au(tpy)$(OAc^F)_2$, and consistent with the formation of **3** during the catalytic cycle, the mechanism which had been obtained with ethylene was the foundation for computations using acetylene instead. This mechanism is a two-step process in which an associative substitution of $^{-}OAc^F$ by the substrate is followed by external nucleophilic addition (Scheme 1, path A). This ligand substitution-nucleophilic addition sequence occurs selectively in the position *trans* to tpy-*N*. However, as was done for ethylene, acetylene insertion *trans* to tpy-*N* as well as *trans* to tpy-*C* were both considered in order to evaluate the energetic differences of changing the substrate (Figure 4).

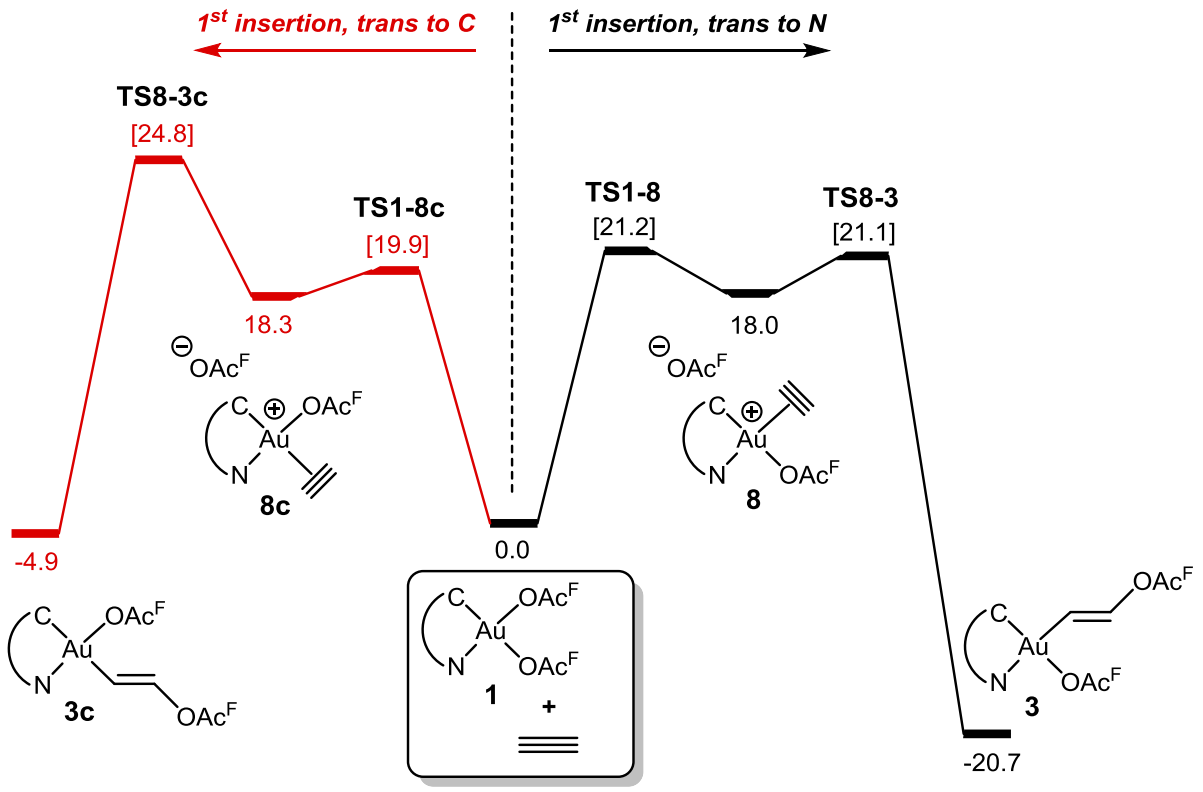

Figure 4. Free energy profile (in kcal mol^{-1}) for the first insertion of acetylene *trans* to tpy-*C* (red) and *trans* to tpy-*N* (black). The energies of all minima and transition states in [brackets] are computed with $HOAc^F$ as the solvent. Transition state geometries for the reaction steps that are inferred to occur (insertion *trans* to tpy-*N*) are shown in Figure 6.

The first step of the reaction, which is the ligand substitution, has a rather similar energy profile when the reaction occurs *trans* to tpy-*N* or *trans* to tpy-*C*, with energies for **8** and **8c** of *ca* 18 kcal mol^{-1}. In contrast, the nucleophilic addition step is kinetically and thermodynamically preferred *trans* to tpy-*N* by 3.7 and 15.8 kcal mol^{-1}, respectively. This is consistent with the observed insertion of acetylene *trans* to tpy-*N* and therefore the spontaneous formation of **3** during the reaction. In addition, this reaction is clearly irreversible since the energy barrier for the reverse process is > 40 kcal mol^{-1}.

As proposed earlier, two scenarios could be envisioned for completion of the catalytic trifluoroacetoxylation of acetylene from **3** after the observed, initial insertion *trans* to tpy-*N*: (1) protolytic cleavage of the Au–vinyl bond (Scheme 4); and (2) insertion of a second molecule of acetylene into the Au–OAc^F bond *trans* to tpy-*C* followed by protolytic cleavage of the resulting Au–vinyl bond (Scheme 7, c and d). These pathways were computationally explored using **3** as the energy base level (Figure 5), since as pointed out above, the formation of this species from **1** is irreversible. Protolytic cleavage of the Au–vinyl bond in **3**, which is *trans* to N, has an energy barrier (**TS3-9**) of 24.8 kcal mol^{-1}. Although this barrier could be

surpassable, it appears too high for a reaction which occurs readily at ambient temperature, and indeed no formation of the expected products **1** and **4** was observed by addition of $HOAc^F$ to **3**. In contrast, the insertion of a second molecule of acetylene, this time *trans* to tpy-*C*, has a somewhat lower energy barrier of 22.7 kcal mol^{-1} (**TS10c-7**). This energy is 2.1 kcal mol^{-1} lower than the same process (**TS8-3c**) from **1**, in which the position *trans* to tpy-*N* is occupied by an OAc^F ligand. This energy difference, combined with the fact that the position *trans* to tpy-*N* is blocked towards insertion at least by the coordination/nucleophilic attack pathway, allows the second insertion, now *trans* to tpy-*C*, and subsequent formation of the unobserved divinyl complex **7**. Protolytic cleavage of the vinyl ligand *trans* to tpy-*C* from **7** has a rather low barrier of 14.3 kcal mol^{-1} (**TS7-11**), which is consistent with the non-accumulation of **7** during the catalytic reaction. This step leads to the formation of **11**, from which substitution of coordinated **4** by the $^-OAc^F$ anion promotes the forward, strongly exergonic reaction and regenerates the activated catalyst **3** (ΔG = -19.7 kcal mol^{-1}, not shown in Figure 5).

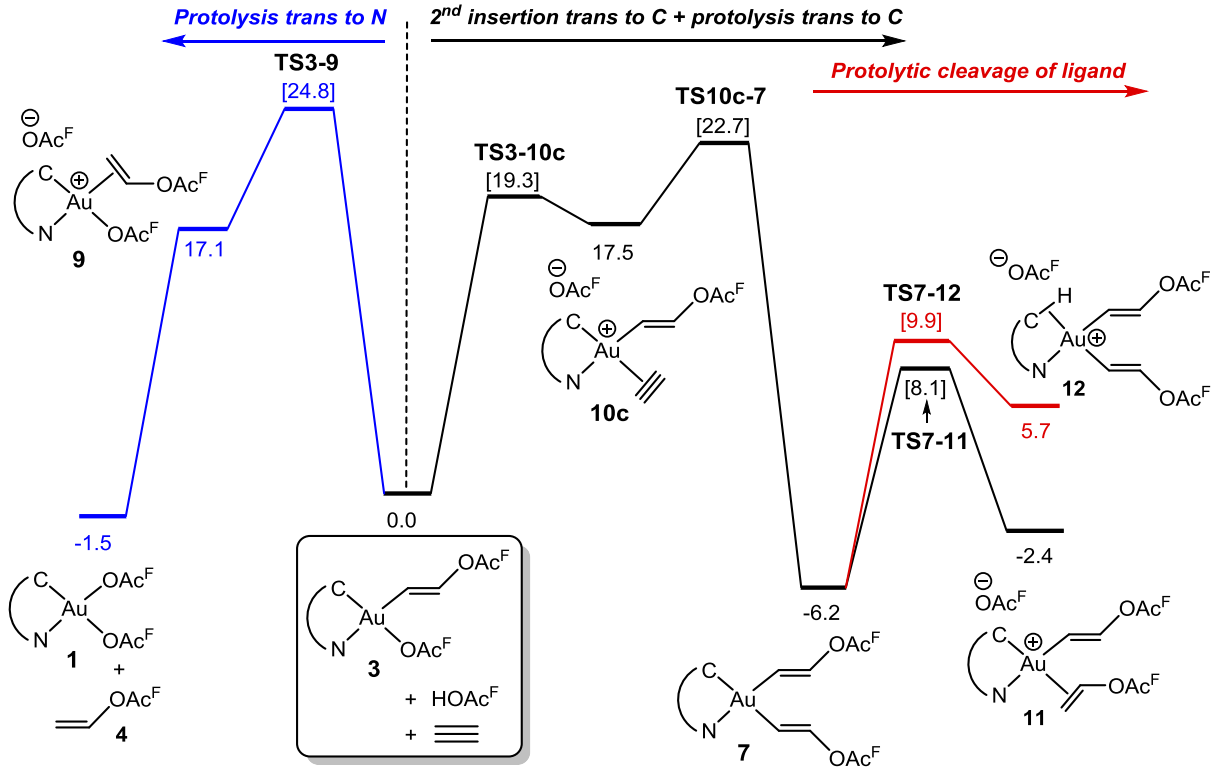

Figure 5. Free energy profile (in kcal mol^{-1}) for the protolytic cleavage of the Au–vinyl bond in **3** (blue), the insertion of acetylene into the Au–OAc^F bond in **3** furnishing **7** followed by protolytic cleavage of the Au–vinyl bond *trans* to tpy-*C* (black), and protolytic cleavage of the Au–C(tpy) bond (red) in **7**. The energies of all minima and transition states in [brackets] are computed in $HOAc^F$. Transition state geometries for the observed reaction steps (reaction *trans* to tpy-*C*) are shown in Figure 6. In order to maintain mass and charge balance, the energies of additional $HOAc^F$, $^-OAc^F$, and/or acetylene have been included in the calculations where needed.

The more facile protolytic cleavage of the Au–vinyl bond *trans* to tpy-*C* (**TS7-11**; $\Delta G^{\ddagger}$ = 14.3 kcal mol^{-1}) compared to the one *trans* to tpy-*N* (**TS7-11c**; $\Delta G^{\ddagger}$ = 26.8 kcal mol^{-1}, not shown in Figure 5) in **7**, can be explained by the higher *trans* effect of the former site of the chelate compared to the latter. In agreement with this, the Au-C(tpy) bond is also prone to be protolytically cleaved in complex **7** since it is *trans* to the vinyl-*C*. The free energy barrier for protolytic cleavage at tpy-*C* is 16.1 kcal mol^{-1} (**TS7-12**), which is *ca* 2 kcal mol^{-1} higher than for the protolytic cleavage of the Au–vinyl bond *trans* to tpy-*C* (**TS7-11**). This difference, albeit small, is consistent with the catalytic hydrotrifluoroacetoxylation of acetylene being preferred (i.e., significant turnover numbers) over catalyst deactivation. Nevertheless, the closeness of the two energy barriers is consistent with the observation of **5** during the catalysis, since formation of the resulting tricoordinated Au(III) species promotes reductive elimination processes.[15,69-73]

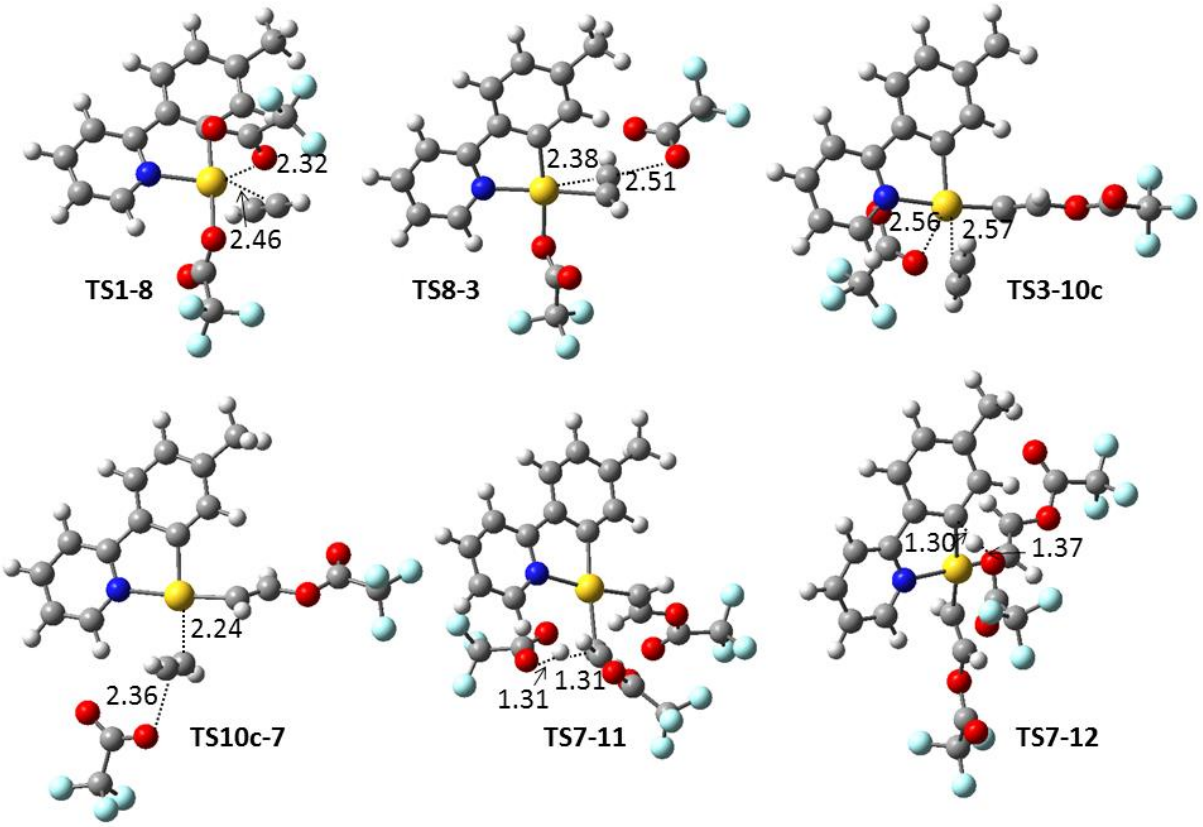

Figure 6. Transition state geometries involved in the reaction of **1** with acetylene. Distances in Å.

Overall, the computational results on the reaction of **1** with acetylene in HOAc^{F} are consistent with the catalytic mechanism proposed in Scheme 7, in which the facile, observed acetylene insertion *trans* to tpy-*N* should be considered to be an activation of the pre-catalyst

1. The catalytic trifluoroacetoxylation reaction takes place *trans* to tpy-*C* in the true catalyst **3**. In order to explain why such catalytic reactivity is not observed with ethylene,[48] the thermodynamics of the three fundamental steps involved in the catalytic cycle, ligand substitution, nucleophilic attack, and protolytic cleavage (A-C in Scheme 10) were computed and compared for the substrates acetylene and ethylene (Table 1). The substitution of an OAc^F ligand by the substrate (step A) shows only small variations in free energy changes for both acetylene and ethylene, in both *trans* to tpy-*N* and *trans* to tpy-*C* positions. By stark contrast, the nucleophilic addition of $^-OAc^F$ (step B) at the substrate bound *trans* to tpy-*N* is more favorable by *ca* 16 kcal mol^{-1} than addition to the substrate bound *trans* to tpy-*C* regardless whether acetylene or ethylene is the substrate. Finally, and importantly, the nucleophilic addition to coordinated acetylene is favored over addition to coordinated ethylene by *ca* 16 kcal mol^{-1}, applicable to reactions *trans* to tpy-*C* as well as *trans* to tpy-*N*. The latter preference was also observed in our recent computational work on the insertion of ethylene and acetylene into Au–X bonds (X = Cl, Me, and H) in simple Au(III) model complexes.[15] The strong thermodynamic preference for nucleophilic addition to acetylene compared to ethylene is the result of two contributing and reinforcing factors. First, there is a lower energy penalty for breaking one π-bond component in a triple bond compared to breaking the π-bond in a double bond. Second, the nucleophilic attack generates a stronger Au–C(sp^2) bond from acetylene than the Au–C(sp^3) bond which results from ethylene.[74] These large energy differences depend on the substrate in question as well as on the position of the bonded substrate (*trans* to tpy-*N* *vs* tpy-*C*) and have remarkable consequences for the insertion reactions (step A + B, Scheme 10). At the position *trans* to tpy-*N*, a *reversible insertion reaction is predicted (and observed*[48]*) with ethylene, but the insertion will be irreversible with acetylene under ambient conditions*. On the other hand, *trans* to tpy-*C*, the insertion is endergonic for ethylene but exergonic for acetylene (*vide infra*). Furthermore, in the ligand protolysis step (C, Scheme 10), the thermodynamics is significantly affected only by whether protolysis occurs *trans* to tpy-*N* or *trans* to tpy-*C*. Protolytic cleavage of the Au-C bond is thermodynamically preferred *trans* to tpy-*C* by *ca* 17 kcal/mol for both acetylene and ethylene, and is exergonic in all cases. Only small variations were observed by changing the other non-tpy ligand (X in Scheme 10 and Table 1) from OAc^F to $CH{=}CHOAc^F$ or $CH_2CH_2OAc^F$.

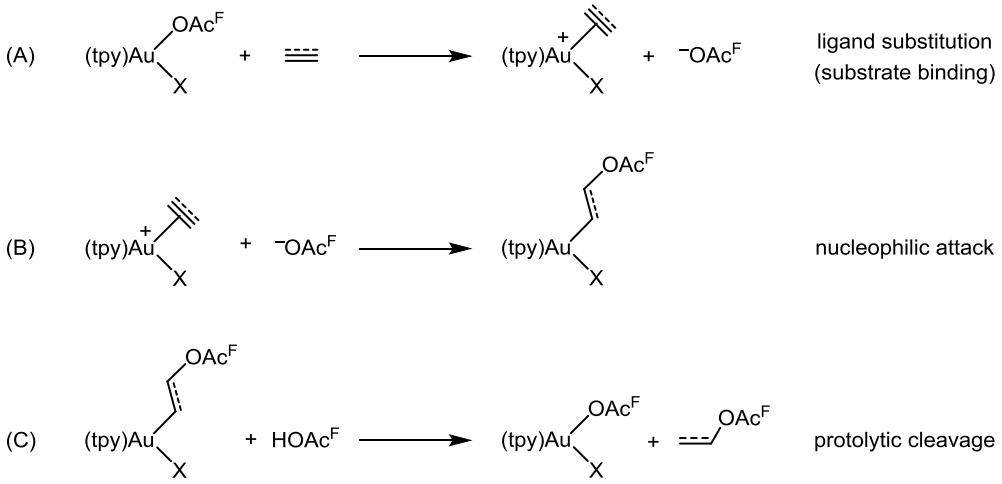

Scheme 10. The three reaction steps for the catalytic trifluoroacetoxylation of acetylene and ethylene. X = OAc^F, $CH{=}CHOAc^F$, or $CH_2CH_2OAc^F$.

Table 1. Calculated free energy changes (kcal mol^{-1}) for reactions (A)-(C) in Scheme 10.[a]

-X =	Reaction	Acetylene		Ethylene	
		rxn *trans* to tpy-*C*	rxn *trans* to tpy-*N*	rxn *trans* to tpy-*C*	rxn *trans* to tpy-*N*
$-OAc^F$	(A)	24.5	23.7	23.6	22.4
	(B)	-29.4	-44.4	-12.5	-29.4
	(C)	-17.3	-1.5	-22.1	-4.0
$-CH{=}CHOAc^F$	(A)	22.0	21.8	–	–
	(B)	-28.3	-43.9	–	–
	(C)	-15.9	-0.1	–	–
$-CH_2CH_2OAc^F$	(A)	_	_	21.3	17.0
	(B)	_	_	-11.7	-25.6
	(C)	_	_	-20.6	-2.5

[a] These values have been computed with the same methodology and without considering ion-pairs to facilitate comparison. Therefore the data may slightly differ from the ones in Figure 4 and 5 and those published in our previous work computed in $HOAc^F$.

The thermodynamic data shown in Table 1 and the kinetics already discussed show that the simple catalytic cycle (single insertion + protonation; Scheme 4) will not proceed

with acetylene. Even though the insertion *trans* to tpy-*N* to give **3** is preferred, kinetically and thermodynamically (and, in practice, is irreversible) over insertion *trans* to tpy-*C* to give **3c** (Figure 4), the protolytic Au–vinyl bond cleavage *trans* to tpy-*N* in **3**, which would complete the cycle, has a higher energy barrier (**TS3-9**, 24.8 kcal mol^{-1}, Figure 5) than the alternative insertion of acetylene *trans* to tpy-*C* in **3** (**TS10c-7**, 22.7 kcal mol^{-1}, Figure 5), which facilitates the observed entry into the more efficient double cycle mechanism.

By contrast, with ethylene, the insertion *trans* to tpy-*N* (previously shown to exhibit reversibility[48]) could in principle, after reversal, allow for the considerably less favorable insertion *trans* to tpy-*C* to furnish **3c-alk** (see Scheme 11), provided that the subsequent protolytic cleavage from this complex could help drive this reaction. However, the computed energy barrier for the protolytic cleavage of the Au-C(sp^3) bond in **3c-alk** (Scheme 11, top) is 23.7 kcal mol^{-1}, which is prohibitively high since the formation of **3c-alk** from **1** is already endergonic by 11.1 kcal mol^{-1} (= $\Delta G^A + \Delta G^B$; data from Table 1, entries for ethylene, X = OAc^F, *trans* to tpy-*C*). Remarkably, when the same reaction was computed from **3c** (Scheme 11, bottom), the energy barrier for the protolytic cleavage of the Au-C(sp^2) bond in **3c** is only 14.5 kcal mol^{-1}. Thus, there is a significant kinetic preference ($\Delta\Delta G^{\neq} \sim 9$ kcal mol^{-1}) for protolysis of the Au–C bond in the Au-CH=$CHOAc^F$ fragment compared to Au-$CH_2CH_2OAc^F$, even though the latter is somewhat more favorable thermodynamically ($\Delta\Delta G° \sim 1.5$ kcal mol^{-1}). This is particularly relevant, because the protolytic cleavages in Scheme 11 must compete favorably with the protolytic cleavage at tpy-*C* in order for catalysis to occur (otherwise, catalyst decomposition takes place, as evidenced by the formation of **5** and H_2tpy^+ observed experimentally). In **7** (Scheme 7), protolysis at the tpy-*C* ligand is less favorable than protolytic cleavage of the vinylic group Au–CH=$CHOAc^F$ (**TS7-12** vs **TS7-11**) *trans* to tpy-*C*. However, the opposite preference is expected in **3c-alk** (Scheme 11), for which protolytic cleavage at tpy-*C* will be favored over $CH_2CH_2OAc^F$. Indeed, as mentioned earlier, we have reported previously that protolytic cleavage at tpy-*C* occurs rapidly even at -60 °C when Au(tpy)Me_2 is treated with trifluoromethanesulfonic acid.[43]

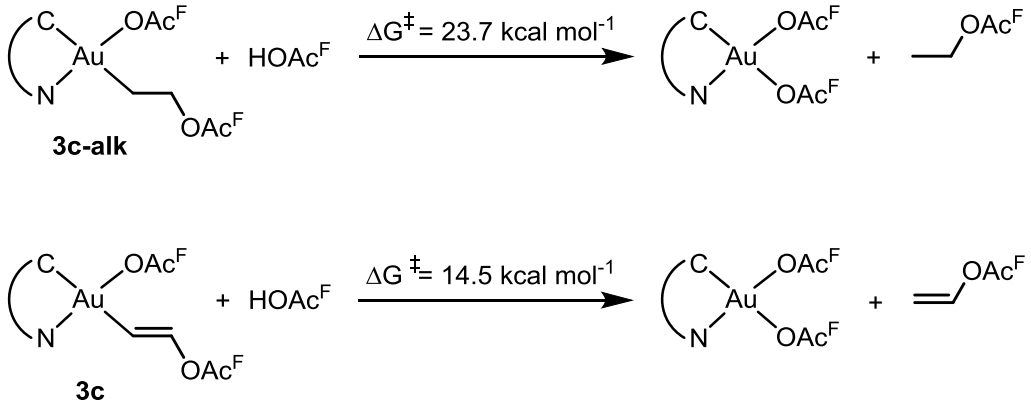

Scheme 11. Protolytic cleavage of Au-C(sp^3) (top) and Au-C(sp^2) (bottom) bonds *trans* to tpy-*C*.

CONCLUSIONS

This study of catalytic acetylene functionalization, combined with our earlier investigation of ethylene insertion reactivity,[48] at Au(tpy)(OAc^F)$_2$ has led to fundamental insight into crucial steps that are involved in the reactivity of C–C double and triple bonds at Au(III). Three fundamental steps are involved in these transformations: (a) substitution of an OAc^F ligand by acetylene vs. ethylene; (b) nucleophilic attack by $^-OAc^F$ at coordinated acetylene vs. ethylene; and (c) protolytic cleavage of the Au–C(sp^3) *vs*. Au–C(sp^2) bonds. Experimental and computational results are in excellent agreement and establish that the thermodynamics and kinetics of each of these steps are profoundly affected by the nature of the coordination site *trans* to where the particular transformation takes place, i.e. *trans* to tpy-*C* vs. *trans* to tpy-*N*. Further elaboration and tuning of the chelating ligand, either of its backbone or substitution pattern, should pave the way towards more active and robust Au(III) catalysts for small-molecule functionalization.

SUPPORTING INFORMATION

Experimental and computational procedures, characterization, crystallographic, and computational data. This material is available free of charge via the Internet at http://pubs.acs.org.

ACKNOWLEDGMENT

We gratefully acknowledge financial support from the Research Council of Norway for funding provided through the Centre of Excellence for Theoretical and Computational Chemistry (CTCC; Grant 179568/V30) and for stipends to AN, EL and MSMH (Grants 185513/I30 and 221801/F20), and the Norwegian Metacenter for Computational Science (NOTUR; Grant nn4654k). DB also thanks the EU REA for a Marie Curie Fellowship (Grant CompuWOC/618303). This work was also supported by COST Action CM1205 CARISMA (Catalytic Routines for Small Molecule Activation). GL thanks EPFL and Swiss National Science Foundation for financial support. Furthermore, we would like to thank Roman Tschentscher, SINTEF Materials and Chemistry, for advice with the catalytic experiments, Osamu Sekiguchi, University of Oslo, for performing the MS experiments, and University of Oslo NMR center for giving us generous access to their NMR instruments.

References

(1) Hashmi, A. S. K. *Chem. Rev.* **2007**, *107*, 3180-3211.

(2) *Modern Gold Catalyzed Synthesis*; Hashmi, A. S. K.; Toste, F. D., Eds.; Wiley-VCH: Weinheim, 2012.

(3) Hashmi, A. S. K.; Hutchings, G. J. *Angew. Chem., Int. Ed.* **2006**, *45*, 7896-7936.

(4) Brooner, R. E. M.; Widenhoefer, R. A. *Angew. Chem., Int. Ed.* **2013**, *52*, 11714-11724.

(5) Dorel, R.; Echavarren, A. M. *Chem. Rev.* **2015**, *115*, 9028-9072.

(6) Schmidbaur, H.; Schier, A. *Organometallics* **2010**, *29*, 2-23.

(7) Yang, W.; Hashmi, A. S. K. *Chem. Soc. Rev.* **2014**, *43*, 2941-2955.

(8) Fürstner, A. *Acc. Chem. Res.* **2014**, *47*, 925-938.

(9) Fensterbank, L.; Malacria, M. *Acc. Chem. Res.* **2014**, *47*, 953-965.

(10) Zhang, L. *Acc. Chem. Res.* **2014**, *47*, 877-888.

(11) Zhang, D.-H.; Tang, X.-Y.; Shi, M. *Acc. Chem. Res.* **2014**, *47*, 913-924.

(12) Krause, N.; Winter, C. *Chem. Rev.* **2011**, *111*, 1994-2009.

(13) Corma, A.; Leyva-Pérez, A.; Sabater, M. J. *Chem. Rev.* **2011**, *111*, 1657–1712.

(14) Rudolph, M.; Hashmi, A. S. K. *Chem. Soc. Rev.* **2012**, *41*, 2448-2462.

(15) Balcells, D.; Eisenstein, O.; Tilset, M.; Nova, A. *Dalton Trans.* **2016**, *45*, 5504-5513.

(16) Liu, L.-P.; Hammond, G. B. *Chem. Soc. Rev.* **2012**, *41*, 3129–3139.

(17) Chiarucci, M.; Bandini, M. *Beilstein J. Org. Chem.* **2013**, *9*, 2586-2614.

(18) Johnston, P.; Carthey, N.; Hutchings, G. J. *J. Am. Chem. Soc.* **2015**, *137*, 14548-14557.

(19) Davies, C. J.; Miedziak, P. J.; Brett, G. L.; Hutchings, G. J. *Chinese J. Catal.* **2016**, *37*, 1600-1607.

(20) Conte, M.; Carley, A. F.; Heirene, C.; Willock, D. J.; Johnston, P.; Herzing, A. A.; Kiely, C. J.; Hutchings, G. J. *J. Catal.* **2007**, *250*, 231-239.

(21) Conte, M.; Carley, A. F.; Attard, G.; Herzing, A. A.; Kiely, C. J.; Hutchings, G. J. *J. Catal.* **2008**, *257*, 190-198.

(22) Conte, M.; Hutchings, G. J. In *Modern Gold Catalyzed Synthesis*; Hashmi, A. S. K., Toste, F. D., Eds.; Wiley-VCH Verlag & Co. KGaA: Weinheim, 2012, p 1-26.

(23) Zhang, H.; Dai, B.; Wang, X.; Xu, L.; Zhu, M. *J. Ind. Eng. Chem.* **2012**, *18*, 49-54.

(24) Tolbert, T. L.; Waddell, W. A., Jr. (Monsanto Co.). U.S. Patent 3177243, **1965**.

(25) Dickey, J. B.; Stanin, T. E. (Eastman Kodak Co.). U.S. Patent 2525530, **1950**.

(26) Ranieri, B.; Escofet, I.; Echavarren, A. M. *Org. Biomol. Chem.* **2015**, *13*, 7103-7118.

(27) Kumar, R.; Nevado, C. *Angew. Chem., Int. Ed.* **2017**, *56*, 1994-2015.

(28) Henderson, W. *Adv. Organomet. Chem.* **2006**, *54*, 207-265.

(29) Huang, L.; Rominger, F.; Rudolph, M.; Hashmi, A. S. K. *Chem. Commun.* **2016**, *52*, 6435-6438.

(30) Roth, T.; Wadepohl, H.; Gade, L. H. *Eur. J. Inorg. Chem.* **2016**, *2016*, 1184-1191.

(31) Wang, Q.; Jiang, Y.; Sun, R.; Tang, X.-Y.; Shi, M. *Chem. Eur. J.* **2016**, *22*, 14739-14745.

(32) Wu, C.-Y.; Horibe, T.; Jacobsen, C. B.; Toste, F. D. *Nature* **2015**, *517*, 449-454.

(33) Kawai, H.; Wolf, W. J.; DiPasquale, A. G.; Winston, M. S.; Toste, F. D. *J. Am. Chem. Soc.* **2016**, *138*, 587-593.

(34) Hofer, M.; Nevado, C. *Eur. J. Inorg. Chem.* **2012**, *2012*, 1338-1341.

(35) Ball, L. T.; Lloyd-Jones, G. C.; Russell, C. A. *J. Am. Chem. Soc.* **2014**, *136*, 254–264.

(36) Hopkinson, M. N.; Gee, A. D.; Gouverneur, V. *Chem. Eur. J.* **2011**, *17*, 8248-8262.

(37) Wang, W.; Jasinski, J.; Hammond, G. B.; Xu, B. *Angew. Chem., Int. Ed.* **2010**, *49*, 7247-7252.

(38) de Haro, T.; Nevado, C. *Adv. Synth. Catal.* **2010**, *352*, 2767-2772.

(39) Peng, Y.; Cui, L.; Zhang, G.; Zhang, L. *J. Am. Chem. Soc.* **2009**, *131*, 5062-5063.

(40) Zhang, G.; Peng, Y.; Cui, L.; Zhang, L. *Angew. Chem., Int. Ed.* **2009**, *48*, 3112-3115.

(41) Cinellu, M. A.; Minghetti, G.; Cocco, F.; Stoccoro, S.; Zucca, A.; Manassero, M. *Angew. Chem., Int. Ed.* **2005**, *44*, 6892-6895.

(42) Liu, Y.; Chen, X.; Zhang, J.; Xu, Z. *Synlett* **2013**, *24*, 1371-1376.

(43) Langseth, E.; Scheuermann, M. L.; Balcells, D.; Kaminsky, W.; Goldberg, K. I.; Eisenstein, O.; Heyn, R. H.; Tilset, M. *Angew. Chem., Int. Ed.* **2013**, *52*, 1660-1663.

(44) Savjani, N.; Roşca, D.-A.; Schormann, M.; Bochmann, M. *Angew. Chem., Int. Ed.* **2013**, *52*, 874-877.

(45) Rekhroukh, F.; Estevez, L.; Bijani, C.; Miqueu, K.; Amgoune, A.; Bourissou, D. *Organometallics* **2016**, *35*, 995-1001.

(46) Pernpointner, M.; Hashmi, A. S. K. *J. Chem. Theory Comput.* **2009**, *5*, 2717-2725.

(47) Lein, M.; Rudolph, M.; Hashmi, A. S. K.; Schwerdtfeger, P. *Organometallics* **2010**, *29*, 2206-2210.

(48) Langseth, E.; Nova, A.; Tråseth, E. A.; Rise, F.; Øien, S.; Heyn, R. H.; Tilset, M. *J. Am. Chem. Soc.* **2014**, *136*, 10104-10115.

(49) Rekhroukh, F.; Estévez, L.; Bijani, C.; Miqueu, K.; Amgoune, A.; Bourissou, D. *Angew. Chem., Int. Ed.* **2016**, *55*, 3414-3418.

(50) Rekhroukh, F.; Estevez, L.; Mallet-Ladeira, S.; Miqueu, K.; Amgoune, A.; Bourissou, D. *J. Am. Chem. Soc.* **2016**, *138*, 11920-11929.

(51) Rekhroukh, F.; Brousses, R.; Amgoune, A.; Bourissou, D. *Angew. Chem., Int. Ed.* **2015**, *54*, 1266-1269.

(52) Rezsnyak, C. E.; Autschbach, J.; Atwood, J. D.; Moncho, S. *J. Coord. Chem.* **2013**, *66*, 1153-1165.

(53) Holmsen, M. S. M.; Nova, A.; Balcells, D.; Langseth, E.; Øien-Ødegaard, S.; Tråseth, E. A.; Heyn, R. H.; Tilset, M. *Dalton Trans.* **2016**, *45*, 14719-14724.

(54) Raubenheimer, H. G.; Schmidbaur, H. *J. Chem. Educ.* **2014**, *91*, 2024-2036.

(55) Egorova, O. A.; Seo, H.; Kim, Y.; Moon, D.; Rhee, Y. M.; Ahn, K. H. *Angew. Chem., Int. Ed.* **2011**, *50*, 11446-11450.

(56) Pintus, A.; Rocchigiani, L.; Fernandez-Cestau, J.; Budzelaar, P. H. M.; Bochmann, M. *Angew. Chem., Int. Ed.* **2016**, *55*, 12321-12324.

(57) Melchionna, M.; Nieger, M.; Helaja, J. *Chem. Eur. J.* **2010**, *16*, 8262-8267.

(58) Lauterbach, T.; Asiri, A. M.; Hashmi, A. S. K. *Adv. Organomet. Chem.* **2014**, *62*, 261-297.

(59) Roşca, D.-A.; Smith, D. A.; Hughes, D. L.; Bochmann, M. *Angew. Chem., Int. Ed.* **2012**, *51*, 10643-10646.

(60) The crystal system of **3** was initially assumed to be base-centered orthorhombic, but during reflection analysis no appropriate orthorhombic space group could be found. Neither could any meaningful crystal structure could be obtained. After careful analysis, the true Bravais lattice was found to be primitive monoclinic, but with cell parameters $a \approx c$ thus emulating the *c*-centered orthorhombic lattice. In addition, all of the examined crystals were twinned by reticular pseudomerohedry via a twofold rotation about the ac face diagonal axis.

(61) Langseth, E.; Görbitz, C. H.; Heyn, R. H.; Tilset, M. *Organometallics* **2012**, *31*, 6567-6571.

(62) Allen, F. H.; Kennard, O.; Watson, D. G.; Brammer, L.; Orpen, A. G.; Taylor, R. *J. Chem. Soc., Perkin Trans. 2* **1987**, S1-S19.

(63) Fan, D.; Melendez, E.; Ranford, J. D.; Lee, P. F.; Vittal, J. J. *J. Organomet. Chem.* **2004**, *689*, 2969-2974.

(64) Venugopal, A.; Shaw, A. P.; Törnroos, K. W.; Heyn, R. H.; Tilset, M. *Organometallics* **2011**, *30*, 3250-3253.

(65) Rupprecht, A. *Acta Chem. Scand.* **1962**, *16*, 2189-2194.

(66) Pinter, B.; Van Speybroeck, V.; Waroquier, M.; Geerlings, P.; De Proft, F. *Phys. Chem. Chem. Phys.* **2013**, *15*, 17354-17365.

(67) *Gold Nanoparticles for Physics, Chemistry and Biology*; Louis, C.; Pluchery, O., Eds.; Imperial College Press, 2012.

(68) Bond, G. C.; Louis, C.; Thompson, D. T. *Catalysis by Gold*; Imperial College Press: London, 2006.

(69) Komiya, S.; Albright, T. A.; Hoffmann, R.; Kochi, J. K. *J. Am. Chem. Soc.* **1976**, *98*, 7255-7265.

(70) Scott, V. J.; Labinger, J. A.; Bercaw, J. E. *Organometallics* **2010**, *29*, 4090-4096.

(71) Mankad, N. P.; Toste, F. D. *Chem. Sci.* **2012**, *3*, 72-76.

(72) Joost, M.; Zeineddine, A.; Estévez, L.; Mallet−Ladeira, S.; Miqueu, K.; Amgoune, A.; Bourissou, D. *J. Am. Chem. Soc.* **2014**, *136*, 14654-14657.

(73) Winston, M. S.; Wolf, W. J.; Toste, F. D. *J. Am. Chem. Soc.* **2014**, *136*, 7777-7782.

(74) Clot, E.; Mégret, C.; Eisenstein, O.; Perutz, R. N. *J. Am. Chem. Soc.* **2006**, *128*, 8350-8357.

Table of Contents entry